A Journal of the Gesellschaft Deutscher Chemiker

Angewandte International Edition GDCh Chemie

www.angewandte.org

Accepted Article

Title: Non-invasive Regulation of Cellular Morphology Using a Photoswitchable Mechanical DNA Polymer

Authors: Soumya Sethi, Kumi Hidaka, Hiroshi Sugiyama, and Masayuki Endo

To be cited as: *Angew. Chem. Int. Ed.* 10.1002/anie.202105425

Link to VoR: https://doi.org/10.1002/anie.202105425

WILEY-VCH

10.1002/anie.202105425

WILEY-VCH

FULL PAPER

Non Invasive Regulation of Cellular Morphology Using a Photoswitchable Mechanical DNA Polymer

Soumya Sethi, [a] Kumi Hidaka, [a] Hiroshi Sugiyama,* [a][b] and Masayuki Endo*[a][b][c]

[a] S. Sethi, K. Hidaka, Prof. Dr. H. Sugiyama, Prof. Dr. M. Endo
Department of Chemistry, Graduate School of Science
Kyoto University
Yoshida-ushinomiyacho, Sakyo-ku, Kyoto 606-8501, Japan
E-mail: endo@kansai-u.ac.jp; hs@kuchem.kyoto-u.ac.jp
[b] Prof. Dr. M. Endo, Prof. Dr. Sugiyama
Institute for Integrated Cell-Material Sciences
Kyoto University
[c] Prof. Dr. M. Endo
Organization for Research and Development of Innovative Science and Technology
Kansai University

Supporting information for this article is given via a link at the end of the document.

Abstract: The extracellular matrix, residing the cells provides a dynamic and reversible environment. Spatiotemporal cues are essential when cells are undergoing morphogenesis, repair and differentiation. Recapitulation of such an intricate system with reversible presentation of nanoscale cues can help us better understand cellular processes and can allow precise manipulation of cell function in vitro. Herein, we formulated a photoswitchable DNA mechanical nanostructure containing azobenzene moieties and dynamically regulated the spatial distance between adhesion peptides using the photoswitchable DNA polymer with photoirradiation. We found that the DNA polymer reversibly forms two different structures, a relaxed linear and shrinked compact form, observed by AFM. Using mechanical properties of this DNA polymer, UV and visible light irradiation induced significant morphology change of cells between a round shape and spindle shape, thus provides a tool to decipher the language of the ECM better.

Introduction

Cells in their native microenvironment receive signals dynamically, reversibly and synergistically. The extracellular environment that surrounds the cells has a unique composition and topology and regulates crucial cellular processes like cell adhesion, migration, proliferation and differentiation through a reciprocal and reversible dialogue between various cellular components and receptors.[1,2] To artificially mimic the extracellular environment, it is imperative to emulate the nanoscale precision of the native microenvironment along with the dynamic and reversible nature of the matrix. Current existing techniques mostly provide static cell adhesions[3] or non-reversible dynamic substrates.[4,5]DNA is considered as an ideal candidate to form highly programmable nanostructures due to its property of sequence-specific hybridization.[6] Previous reports have shown that DNA can form extracellular matrix (ECM) like scaffolds effectively for instance DNA nanoribbons decorated with cell adhesion peptides,[7] nanotubes labelled with cell binding peptides,[8] DNA origami nanoarrays,[9] nanocalipers,[10] DNA based hydrogels[11] etc. which have been shown to support cell adhesion, growth, proliferation and differentiation. These systems mimic nanoscale cues provided for the cells but lack in providing a dynamic and reversible environment with a spatio-temporal control. Recent reports display the use of strand displacement controlled DNA nanomachines[12,13] to effect the cellular morphology. Such DNA nanomachines involve DNA hybridization reactions, which tend to consume molecular fuels for each cycle and thereby leading to accumulation of unwanted molecular waste in the reaction mixture, providing only a temporal control and thus, limiting the reversibility and efficiency of the system.

Controlling the changes by employing external stimuli like photoirradiation can help overcome the challenges faced by the pre-existing methods. Photocontrol can add another dimension of control to the existing system i.e. a spatial control. A photoresponsive DNA coupled with azobenzene moieties has been reported to reversibly control hybridization and dehybridization of the DNA strands caused by switching between the cis/trans state of azobenzene with photoirradiation.[14,15] Using this system as a principle of design, photocontrolled DNA nanodevices were constructed for biological applications. [16,17]

In this study, we designed a photoresponsive mechanical DNA polymer that can dynamically and reversibly cause a displacement of the cell adhesion peptides (RGD) (Figure 1). The photoresponsive DNA polymer with azobenzene photoswitches were designed to reversibly form a relaxed linear and shrinked compact structure depending on the photoirradiation wavelengths. Using this DNA polymer as an ECM, we reversibly regulate the morphology change of the cells from a spindle shaped morphology with few stress F-actin fibres to a rounder morphology with defined stress F-actin fibres (Figure 1a). The reversible and dynamic change in the distance of the adhesion peptides in the DNA polymer should significantly affect the morphology of the cells and consequent induction of cellular responses, and thus help us provide a spatial and temporal control over the cellular morphology.

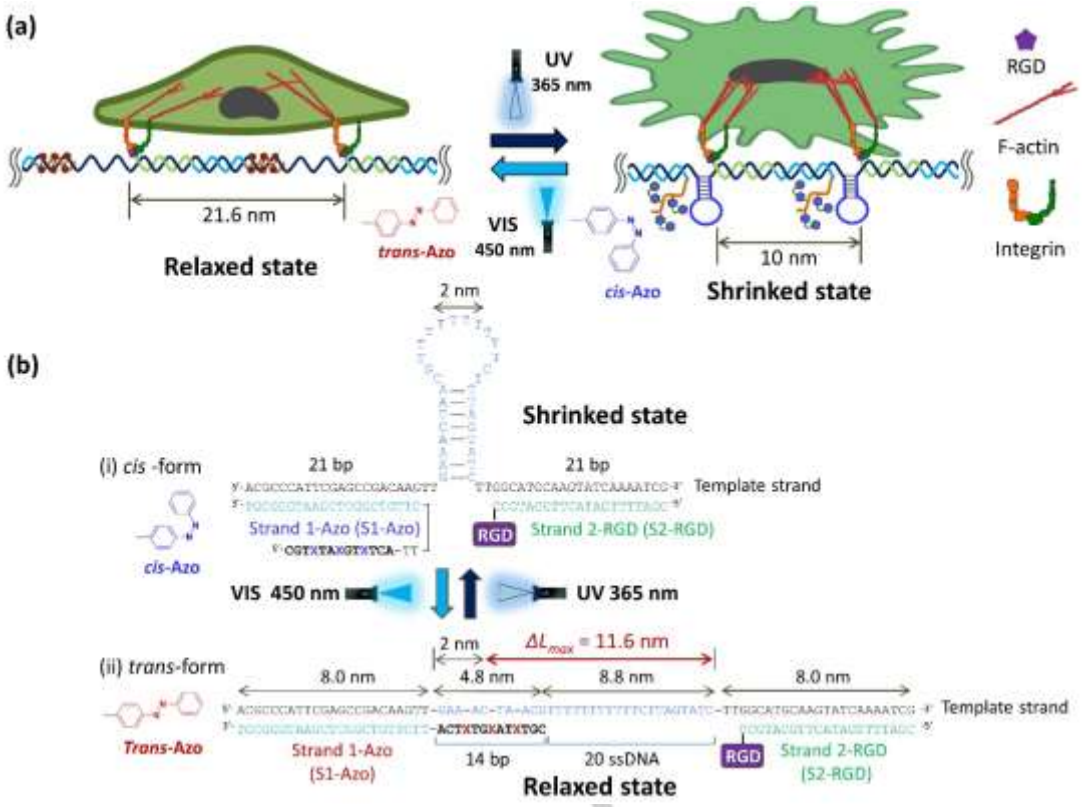

Figure 1. Photoresponsive mechanical DNA polymer for spatial and temporal control of cellular morphology. (a) Schematic diagram of the photoresponsive mechanical DNA polymer depicts the cell morphology change as the conformation of the DNA polymer changes. (b) Design of the DNA component and the predicted conformation and distance change when the DNA component is subjected to UV- VIS irradiation. (i) Hairpin formation is predicted when azobenzenes incorporated in strand 1 (S1-Azo) are in cis conformation. (ii) Disruption of the hairpin and hybridization of S1-Azo (trans-form) upon VIS irradiation.

Results and Discussion

Design of the photocontrolled mechanical DNA polymer

We designed a DNA component structure to control the distance between the cell adhesion peptides, which was inspired by a previous report. [12] We introduced azobenzene moieties in one DNA strand labelled as Strand1-Azo (S1-Azo). To perform photocontrolled conformational change of the component, the DNA component forms a linear structure under visible (VIS) light, where the azobenzene moieties take the *trans* conformation for hybridization, whereas under UV light the azobenzene moieties take the *cis* conformation for dehybridization and consequently the hairpin formation occurs in the template strand (Figure 1b). The DNA component structure was also designed to cause a reversible change in the conformation by photoirradiation. This conformational change of the DNA component can induce 11.6 nm expansion and shrinking in length between the two states. The switching efficiency of hybridization and dehybridization using azobenzene-containing strands has been reported in >85% yield, [14,15] so we expect the reversible conformational change with UV and VIS irradiation.

Studying the shrinking and relaxation of the photocontrolled mechanical DNA structure

To characterize the conformational change of the photoresponsive DNA component, we performed the gel electrophoresis and AFM observation. The conformational change was detected by the shift of the bands in the native PAGE gel (Figure 2a). The initial structure was formed with S1-Azo (*trans*-form), S2, and complementary strand by annealing, and migrated as a single band in the gel (lane 3). Next, we used UV irradiation (365 nm, 37°C for 10 min) to induce conformational change of the structure. Interestingly, after UV irradiation, the bands of the formed structure appeared multiple and migrated slower (lane 4), indicating that the DNA component with *cis*-azobenzenes tended to interact each other and formed multiple structures. DNA assembly formed using UV irradiated S1-Azo (*cis*-form) also showed the same pattern of migration bands in the gel (lane 2). The single-stranded *cis*-azobenzene strand in S1-Azo may interact with single-stranded hairpin loop part of another component, thus the existence of the lower mobility bands in the UV irradiated samples. After VIS irradiation (450 nm, 37°C for 10 min), the lower mobility bands completely disappeared and returned to the initial band (lane 5). Although the conformation of the DNA component in *cis*-form is unclear, the reversibility of the conformations of the DNA component and the interaction can be controlled by switching of photoisomerization of azobenzene moieties with UV and VIS irradiation.

Next, to further characterize the conformational change in solution, we used a FAM/Dabcyl fluorescence quenching system (Figure S2). The template strand (76-nt) was consecutively hybridized with an FAM-labelled Strand 2 (F-S2, fluorophore) and a UV irradiated (37°C for 10 min) dabcyl-labelled Strand 1-Azo (Q-S1-Azo, quencher). This annealed product was then UV irradiated (37°C for 10 min). After UV irradiation, the fluorescence intensity decreased by 14%, showing that the quenching occurred

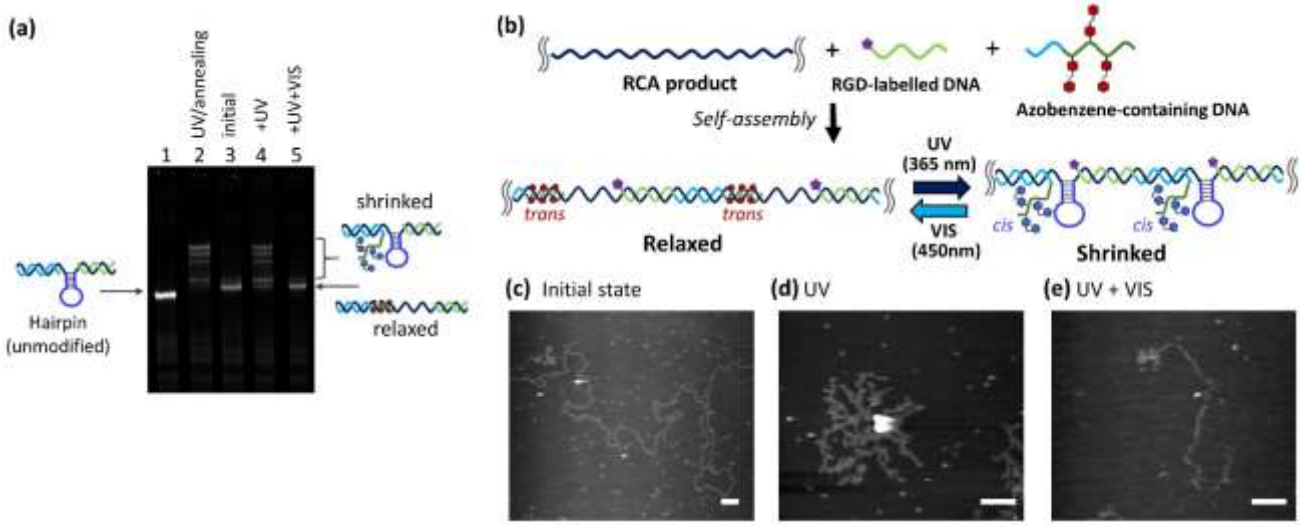

Figure 2. Reversible conformational change of Azo-containing DNA component induced by the photoisomerization with UV/VIS irradiation. (a) Photocontrol mechanical switching of the DNA component structure with UV-VIS irradiation. 15%-native PAGE gel was used for the characterization of the conformation of the DNA component upon UV and VIS irradiation. (b) A long DNA sequence generated using rolling circle amplification (RCA) was used as a template to assemble the photoresponsive DNA strand (S1-Azo) and RGD-labelled strand (S2-RGD). (c) AFM image of initial state of the DNA polymer after annealing with RCA product, S1-Azo and S2-RGD. (d) AFM image of DNA polymer after UV irradiation. (e) AFM image of DNA polymer after sequential UV and VIS irradiation. Scale bar: 100 nm

by approaching the FAM and quencher in the shrinked state. The quenching efficiency was not strong enough maybe because the position to introduce the quencher was fixed in the internal strand and was not optimized. After VIS irradiation (37°C for 10 min), the fluorescence intensity recovered, indicating that the conformation returned to the relaxed state. Moreover, this DNA component could continuously cycle between the two states, cyclic conversion of the two states is depicted in Figure S2, and it is shown that the component structure could continuously cycle between the linear and hairpin states. Although the signal strength reduction seems lower than expected, we could obtain distinct and reversible migration on the gel, showing that our DNA component could be employed for the further polymerization to prepare a photoresponsive mechanical DNA polymer.

Reversibility of the photocontrolled mechanical DNA polymer

We next prepared a photoresponsive DNA polymer using a long scaffold strand prepared by rolling circle amplification (RCA) (Figure 2b). The size of the RCA product was estimated to be around 15,000 bp from the gel and the AFM images (Figure S1). The long scaffold was annealed with the complementary strands (S1-Azo and S2) at 85 °C to 15°C at a rate of -1.0 °C /min in a buffer containing 20 mM Tris-HCl (pH 7.6), 5 mM $MgCl_2$ and 50 mM NaCl. The molar ratio of RCA product and S1-Azo was 1:200 to study the contraction and relaxation in an amber coloured tube to protect the azobenzene strand from light.

The sample was divided into three parts; Sample 1 – relaxed state whereby observations were made immediately after annealing the mixture; Sample 2 – shrinked state whereby UV was irradiated at 37°C for 10 min; Sample 3 – re-relaxed state whereby UV, followed by VIS was irradiated at 37°C for 10 min. All the samples were observed using high-speed AFM (Figure 2c-e). Figure 2c represents AFM image of the initial state of the DNA polymer after assembling. We observed a long linear structure with flexibility. Then after UV-irradiation, the DNA polymer was observed as a shrinked nanostructure (Figure 2d), which also contained confined hairpin-like structures in the polymer strand (Figure S3). Interestingly, the shrinked structure seems more compact than expected, suggesting that the azobenzene-containing DNA strands interacted weakly to form a two-dimensional structure. Such an interaction was also observed in migration bands of the DNA component in the native PAGE gel (Figure 2a). As observed here, there was a clear demarcation in the conformations of the relaxed and shrinked nanostructures. Then after VIS irradiation, the DNA polymer reverted back to a linear structure (Figure 2e). These results indicate that the extension and shrinking of the DNA polymer occurred clearly by UV and VIS irradiation. Since UV irradiation induced a formation of a compact structure, we predict this occurrence is due to the interactions of the azobenzene-containing strands that leads to a formation of a compact mesh-like structure. This photoresponsive mechanical DNA polymer was further used for the regulation of cellular morphology.

Photocontrolled mechanical DNA polymer with multivalent cell binding peptides

To facilitate cell binding and spreading onto the formulated mechanical DNA polymer, it was then hybridized to RGD [Cyclo(-RGDfK)] conjugated Strand 2 (S2-RGD). RGD is the peptide sequence known to be a part of the cell binding domain of fibronectin[18] and is shown to have an effective cell binding activity through integrin receptors in many biomaterials.[7,8] The peptide was conjugated to the DNA using a heterobifunctional linker sulfo-SMCC and subsequently the peptide conjugated DNA was purified using HPLC and characterised on a 20% denaturing page gel (Figure S1c). We next set out to investigate the presence of the RGD onto the DNA polymer, and the adhesion of HeLa cell line was studied on the relaxed DNA polymer coated surfaces. The molar ratio of RCA product: RGD was kept as 1:50. HeLa was chosen as the test cell line because of its highly adherent capabilities. As a negative control, only RCA product-coated surfaces were chosen and as a positive control HeLa cells plated on a cell culture dish (regular cell attachment as control) was

10.1002/anie.202105425

chosen. After, the attachment and spreading of the cells, the cells were then fixed and stained with an F-actin stain and a nucleus stain and visualized under a confocal microscope. The area occupied by the cells was analyzed using Image J when seeded on each of the substrates. As shown in the Figure S4, the cells readily adhered on all the three substrates but the cell spreading was evidently more in case of RCA product/S2-RGD (1:50) when compared with only RCA product coated surface. This observation suggests that S2-RGD was successfully hybridized to the RCA product and that the presence of RGD on the DNA polymer allowed cells to spread and adhere well.

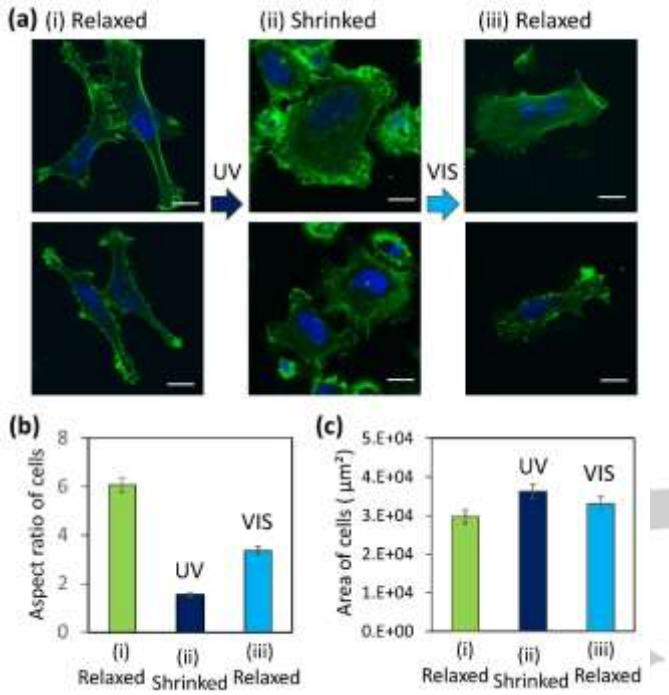

Figure 3. Spatial and Temporal photocontrol of HeLa cell morphology. Photocontrol mechanical switching of DNA Polymer to regulate cell morphology. (a) Representative images of HeLa cells cultured on three different states of the DNA polymer (relaxed, shrinked, re-relaxed) after 9 h of cell culture. Cell nuclei are stained in blue (DAPI staining) and F-actin is stained in green (FITC-labelled phalloidin staining). Scale bar: 10 µm. (b)(c) Aspect ratio of cells and area occupied by the cultured cell on the three substrates were measured and calculated using Image J. Fifty cells were analysed for each sample. Error bars (SD) are based on three independent experiments.

Reversible control of HeLa cell morphology using the photoresponsive mechanical DNA polymer

We next investigated the effect of the shrinking and relaxation of the photoresponsive mechanical DNA polymer on HeLa cells. A previous report showed that the morphology of HeLa cells could be regulated using the DNA nanostructure, [12] in which the DNA nanostructure uses DNA hybridization reaction to cause extension and contraction. However, the strand displacement reaction requires the addition of fuel strands each time to induce the conformational changes, which can only be achieved by changing the media, thus not only does it limit repeatability but also can compromise with sterility. Furthermore, although the existing system provides us useful insights in the cell membrane receptor functionality, lags in a spatio-temporal control over the cellular morphology thus limits in emulating the dynamics of the extracellular matrix.

Using our photoresponsive mechanical DNA polymer, we aim to formulate a biomaterial which can provide a spatial and temporal control over the cellular morphology using photo-irradiation. Wavelengths of 365 nm and 450 nm have been reported to cause no harm to cells when used in a controlled intensity and for a controlled time. [19] We performed photo-toxicity studies on both HeLa and human mesenchymal cells used in this study to rule out any possibility of cell damage or death by UV or UV morphogenesis (Figure S10 to Figure S14). We observed no negative effects of UV (365nm) for the desired time at constant temperature on the cells. Thus, we set out to use UV irradiation (365 nm) as it can be provided to the cells over the culture plate to the designed area, with no compromise in sterility and almost no loss in repeatability can be achieved.

To confirm our hypothesis, we used HeLa cells for the initial experiments. Based on our previous results, the length of the RCA scaffold could be estimated to 200 repeat units, thus, the molar ratios of RCA scaffold: S1-Azo was 1:200 and molar ratio of RCA scaffold: S2-RGD was 1:50 to cause a significant amount of change in the cell morphology when the conformation of the DNA polymer changed. It is imperative to understand that the changes in distances might vary from as shown in Figure 1a in each cycle, as the polymer is a highly flexible DNA scaffold, but we hypothesize from the previous reports[12] that these changes should be good enough to cause a change in the cell morphology.

Firstly, we ensured the stability of the coated DNA polymer on 3-aminopropyltriethoxysilane (APTES)-modified glass in the cell culture media used for the experiments. We incorporated S2-FAM within the DNA polymer to observe the coating under a confocal microscope. We observed the DNA polymer coating at various time intervals to ensure no degradation during time period of our experiment (Figure S8). We observed that until 24 h there was no loss in fluorescence intensity of FAM, and after 48h there seemed decrease of FAM intensity. Thus, we could conclude that our DNA polymer coating in the extracellular environment was stable for at least 24h. We confirm that DNA polymer can maintain its integrity for atleast 24 h in the culture medium.

We next checked the presence of cells on the DNA polymer and ensure that the cells are adhered on the DNA polymer-coated glass during the duration of the experiment. For this experiment, we annealed RCA product with S1-Azo, S2-RGD, and S2-FAM (in equal molar ratios) and coated it onto APTES-modified glass. After thorough washing, HeLa cells were seeded onto the DNA polymer-coated substrates and incubated in the presence of culture media. The coating and cells seeded onto it was observed at various time points (Figure S9). It was observed that cells remained well attached onto the DNA polymer for at least 24 h. Thus, the DNA polymer maintained its existence in the extracellular environment and the cells remained well attached onto it during the entire experiment duration. After these initial experiments, we proceeded to check the photo-switching of the DNA polymer.

HeLa cells were seeded on the DNA polymer-coated substrates, where all the substrates were initially coated by the relaxed DNA polymer (Figure 3 and S5). After 3 h of seeding, the specific areas were irradiated by UV light (10 min at 37 °C) to cause shrinking and tension of the DNA polymer. After next 3 h, the specific areas were irradiated by VIS light (10 min at 37 °C) to cause re-relaxation of the DNA polymer. A clear difference in the cellular morphology was observed on the cells cultured on the relaxed DNA polymer, where the HeLa cells appear to be well

aligned and long in shape (Figure 3a(i) and S5), whereas after UV irradiation, the cells appear to be less aligned, rounder in appearance and better spread (Figure 3a(ii) and S5), so the changes in spreading of the cells were very significant. Further, it was seen that upon irradiation of VIS light the cell morphology reversed back to the relaxed morphology (Figure 3a(iii) and S5). The changes in the morphology were characterized by aspect ratio of cells and area (Figure 3b and 3c), which show that the shrinking and expansion of the cells occurred reversibly upon photoirradiation. Thus, changing the distance between the RGD peptides in the DNA polymer led to a reversible change in the cell morphology, including cell spreading and actin remodelling.

We next set out to confirm that these changes in the morphology are due to changes in the distance of RGD peptides in DNA polymer and not caused by UV irradiation or any another element in the experiment, thus we established control experiments. Firstly, instead of S1-Azo, we used only S1 in the formation of the DNA polymer, so as to form a static shrinked DNA polymer which cannot change shape upon UV or VIS irradiation. We next investigated the morphology under initial conditions and UV irradiation conditions for HeLa cells (Figure S15) and observed that the cells did not undergo a morphology change even after UV irradiation and area occupied by the cells was calculated and compared. Next, we wanted to further confirm this and designed another control experiment using human mesenchymal stem cells (Figure S16), here we used a non-complementary DNA template, such that even when azobenzene is in trans state, there is no complementarity between S1-Azo and the loop strand, thus allowing the formation of only static shrinked structures. We next coated the formed DNA polymer onto APTES-modified substrates, seeded hMSCs, and investigated the morphologies on the initial and UV-irradiated matrix. After careful observation and analysis, we found no remarkable changes in the cell morphologies. This was further confirmed by aspect ratio comparison of cells between the two states. Thus, this leads us to confirm that the morphology changes observed in the Figure 3 were not caused by the detrimental effects of UV light or any other elements in the experiment and solely due to structural change of DNA polymer.

Reversible control of human Mesenchymal Stem Cell morphology using the photo-responsive mechanical DNA polymer

After observing the reversible effects of shrinking and relaxation of the DNA polymer on our HeLa cell test line, we next set out to investigate its effects on human mesenchymal stem cells (hMSCs). It is well known that mesenchymal stem cells have a tremendous potential for tissue engineering applications and can be differentiated into many lineages, researchers have previously investigated the behaviour of MSCs as influenced by various changes in the extracellular matrix.[20–25] It was clearly demonstrated by the previous experiments [26] that lateral displacement of RGD peptide caused morphology changes in the MSCs, which was further exploited to differentiate the cells. Based on these findings, we considered that a dynamic and reversible system might be able to provide further insights into the understanding of cell morphology changes, cell spreading changes, actin re-modelling, and cell differentiation capabilities.

MSCs were cultured onto the photoresponsive DNA polymer coated surface, which was initially on the relaxed state (Figure S6). Consecutively, the coated surface with MSCs was irradiated with UV light (10 min at 37°C) to achieve the shrinked state and then successively irradiated with VIS light (10 min at 37°C) to form a re-relaxed state (Figure 4 and S7). It was observed that on the relaxed DNA polymer i.e. when the RGD adhesion peptides are spaced farther apart, the cell morphology appears to be spindle shaped and well aligned (Figure 4a(i)). After UV irradiation, the cell morphology appears to be more well spread and rounder because the RGD peptides in the shrinked DNA polymer were relatively close together (Figure 4a(ii)). We also observed significant differences in the organization of actin cytoskeleton. The relaxed state comprised of cells with a disorganized actin cytoskeleton, while the cells on the shrinked state comprised of larger and very well-defined stress fibers (Figure 4a(ii)). After irradiation with VIS light, we observed that the cell morphology reverted back to that of the relaxed state (Figure 4a(iii)). Some of the cells were still in the well spread state, however, majority of the cells reverted to the spindle shape. The changes in the morphology were examined by the change of aspect ratio of cells and area (Figure 4b and 4c), showing that the shrinking and expansion of the cells occurred reversibly. Thus, we could achieve an on-demand reversible control over the cellular morphology. Photocontrol can allow us to specifically alter the morphology in a designated area and has the potential to allow controlled differentiation of MSCs based on the cell shape into different lineages.[26,27]

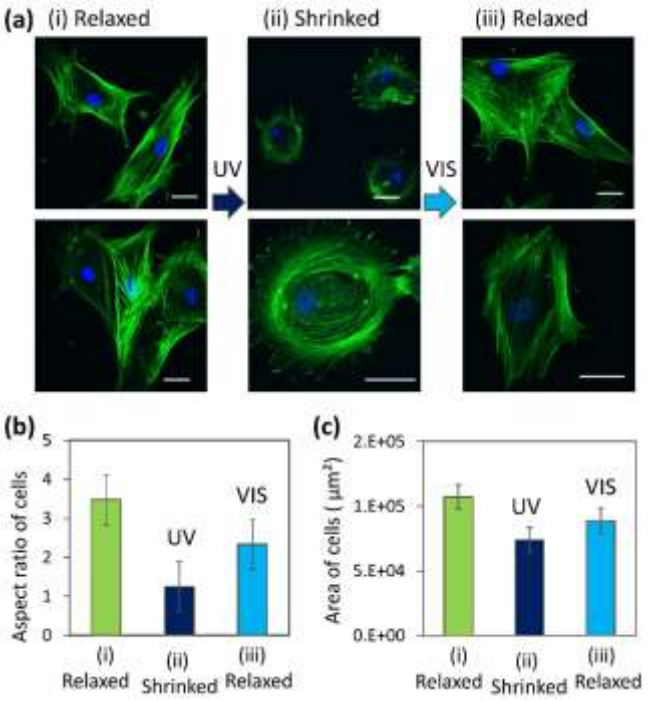

Figure 4. Spatial and Temporal photocontrol of mesenchymal stem cell (MSC) morphology. Photocontrol mechanical switching of DNA polymer to regulate cell morphology. (a) Representative images of MSCs cultured on three different states of the DNA polymer (relaxed, shrinked, re-relaxed state) after 9 h of cell culture. Cell nuclei are stained in blue (DAPI staining) and F-actin is stained in green (FITC-labelled phalloidin staining). Scale bar: 30 μm. (b)(c) Aspect ratio of cells and area occupied by the cultured cell on the three substrates were measured and calculated using Image J. Fifty cells were analysed for each sample. Error bars (SD) are based on three independent experiments.

10.1002/anie.202105425

Repeated cycling between the relaxed and shrinked states

We next examined whether our system could undergo the reversible shrinking and relaxation for more than one cycle without any loss in the efficiency. Similar to the previous experiment, we used hMSCs and seeded them onto the DNA polymer coated substrates (relaxed state) and successively irradiated with 2 cycles of UV and VIS and then fixed, stained and observed the cells (Figure 5). We observed a similar cellular morphology changes between the relaxed, shrinked and re-relaxed states (Figure 5a) as we did after only one cycle of irradiation. The changes in the morphology were similarly observed by the change of aspect ratio of cells and area reversibly (Figure 5b and 5c). Thus, we could conclude that our photoresponsive mechanical DNA polymer caused reversible and dynamic changes in the cellular morphology without any loss in efficiency even with two successive cycles of photoirradiations.

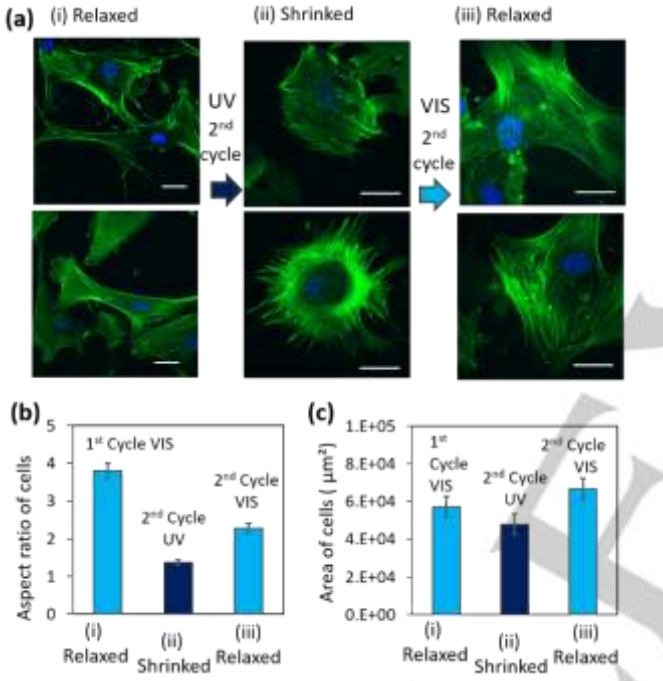

Figure 5. Reversibility of DNA Nanostructure over 2 cycles. Photocontrol mechanical switching of DNA polymer to regulate cell morphology. (a) Representative images of MSCs cultured on three different states of the DNA polymer (second time relaxed, shrinked, re-relaxed) after 18 h of cell culture. Cell nuclei are stained in blue (DAPI staining) and F-actin is stained in green (FITC-labelled phalloidin staining). Scale bar: 30 µm. (b)(c) Aspect ratio of cells and area occupied by the cultured cell on the three substrates were measured and calculated using Image J. One hundred cells were analysed for each sample. Error bars (SD) are based on three independent experiments.

Vinculin Expression Distribution Changes between the shrinked and relaxed states

In the above experiments, we observed that reversible displacement of nanoscale cues led to a morphology change and cytoskeletal re-arrangement of the cells. We further wanted to investigate the implications of these changes on cell-matrix interactions. Vinculin is reported to be a major regulator of cell-matrix adhesions and a core focal adhesion protein that appears in the early stage of focal adhesion formation in the form of dot like adhesion complexes.[29,30] It is known that vinculin is an early stage and crucial characteristic of nascent cell-matrix adhesions.[31] As in our photoswitching system we alternated between the relaxed and shrinked states, we noticed that this alternating system might provide us insights about the cell-matrix interactions. We thus set out to investigate the distribution of vinculin protein in the hMSCs by immunostaining of vinculin protein to better understand vinculin distribution and nascent focal adhesions formed by the cells on the relaxed and shrinked states (Figure 6). From the immunostaining results, it was noted that when hMSCs were on the relaxed matrix, the distribution of vinculin was confined to the nuclear regions and was not seen in the cytoplasmic regions (Figure6a, b (i)). Whereas on the shrinked matrix, the distribution of vinculin expression was not only in the nuclear regions but also distributed widely in the cytoplasm (Figure 6a,b(ii)). We confirmed that vinculin distribution was changed in the cells in a reversible manner (Figure 6a,b (iii)). Further, we quantified the staining results by calculating ratio of area of vinculin expression in a cell to the area of the cell in each state. We observed significant changes in the distribution of vinculin among the 3 states from the quantification analysis (Figure 6c). We also performed quantitative polymerase chain reaction (qPCR) of focal adhesion kinase gene, vinculin gene and paxillin gene, which are key proteins in cell –matrix adhesion and observed some upregulation in the shrinked state (Figure S17). Thus, along with the changes in cell morphology and cell cytoskeleton arrangements, cell–matrix adhesions were also seen to change in cells among the relaxed and shrinked states.

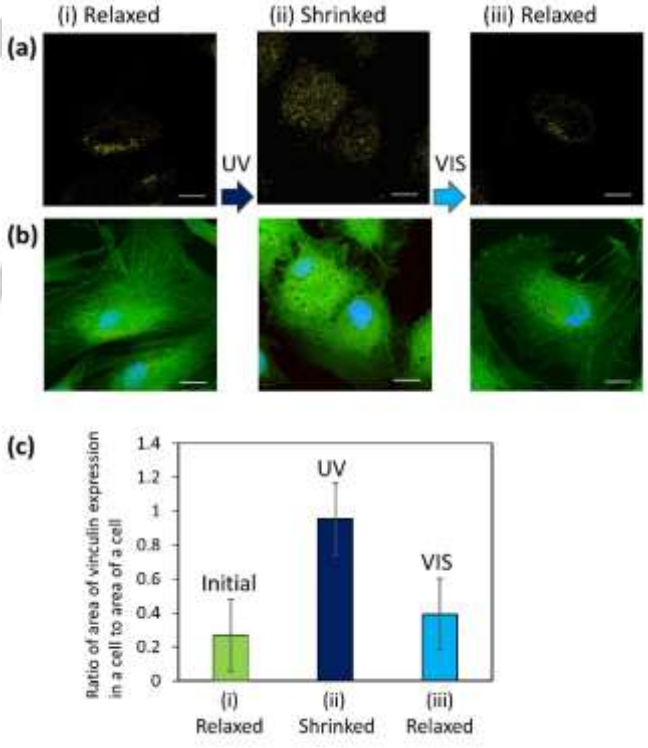

Figure 6. Impact of relaxation and shrinking of DNA polymer as a physical stimulus on cellular adhesion, which was studied using vinculin immunostaining. (a) Representative images of vinculin expression distribution on mesenchymal stem cells (MSCs) cultured on 3 different states of the DNA polymer (relaxed, shrinked, re-relaxed) after 9 h of cell culture. Vinculin was imaged in yellow. (b) Same hMSCs images as above representing co-staining for F-actin (green), cell nuclei (blue; DAPI staining), and vinculin (red). (c) Quantification of immunostaining results by calculating ratio of area of vinculin expression in a cell to the area of the cell in each state. More than 100 cells were observed in each case. (n=3) Scale bar: 20 µm.

Conclusion

We have demonstrated that reversible shrinking and relaxation of the designed photoresponsive mechanical DNA polymer with UV and VIS irradiation. Using HeLa and human mesenchymal stem cells, we found that the photoresponsive mechanical DNA polymer labelled with RGD peptide, which causes a displacement of the RGD ligands, in turn causes the change in the spreading of the cell, the organization of the F-actin filaments, and formation of focal adhesions. Our dynamic and photocontrolled reversible DNA polymer can be used as an efficient and effective tool for understanding many important phenomena such as cell morphogenesis, tissue repair, cancer metastasis, cell differentiation etc. All the above-mentioned phenomenon rely on the basis of cell-cell and cell-substrate attachment. Such an extracellular matrix mimicking dynamic tool is very critical and beneficial in understanding and expanding our knowledge.

Acknowledgements

This work was supported by a Grant-in-Aid for Scientific Research JSPS KAKENHI Fund 16H06356 to HS and ME, and 18KK0139 and to ME. Financial support from the Uehara Memorial Foundation, the Nakatani Foundation, and Heiwa Nakajima Foundation to ME were acknowledged.

Keywords: Cell morphology control • DNA nanotechnology • photo switch • mechanical DNA polymer

References

[1] C. Frantz, K. M. Stewart, V. M. Weaver, *J. Cell Sci.* **2010**, *123*, 4195–4200.

[2] R. O. Hynes, *Science.* **2009**, *326*, 1216–1219.

[3] N. Stephanopoulos, J. H. Ortony, S. I. Stupp, *Acta Mater.* **2013**, *61*, 912–930.

[4] S. Sur, J. B. Matson, M. J. Webber, C. J. Newcomb, S. I. Stupp, *ACS Nano* **2012**, *6*, 10776–10785.

[5] S. J. Todd, D. Farrar, J. E. Gough, R. V. Ulijn, *Soft Matter* **2007**, *3*, 547–550.

[6] O. I. Wilner, I. Willner, *Chem. Rev.* **2012**, *112*, 2528–2556.

[7] F. A. Aldaye, W. T. Senapedis, P. A. Silver, J. C. Way, *J. Am. Chem. Soc.* **2010**, *132*, 14727–14729.

[8] N. Stephanopoulos, R. Freeman, H. A. North, S. Sur, S. J. Jeong, F. Tantakitti, J. A. Kessler, S. I. Stupp, *Nano Lett.* **2015**, *15*, 603–609.

[9] D. Huang, K. Patel, S. Perez-Garrido, J. F. Marshall, M. Palma, *ACS Nano* **2019**, *13*, 728–736.

[10] A. Shaw, V. Lundin, E. Petrova, F. Fördos, E. Benson, A. Al-Amin, A. Herland, A. Blokzijl, B. Högberg, A. I. Teixeira, *Nat. Methods* **2014**, *11*, 841–846.

[11] A. Finke, A. K. Schneider, A. S. Spreng, M. Leist, C. M. Niemeyer, A. Marx, *Adv. Healthc. Mater.* **2019**, *8*, 1–7.

[12] K. Zhang, R. Deng, Y. Sun, L. Zhang, J. Li, *Chem. Sci.* **2017**, *8*, 7098–7105.

[13] R. Freeman, N. Stephanopoulos, Z. Álvarez, J. A. Lewis, S. Sur, C. M. Serrano, J. Boekhoven, S. S. Lee, S. I. Stupp, *Nat. Commun.* **2017**, *8*, 1-11.

[14] X. Liang, T. Mochizuki, H. Asanuma, *Small* **2009**, *5*, 1761–1768.

[15] M. Zhou, X. Liang, T. Mochizuki, H. Asanuma, *Angew. Chemie - Int. Ed.* **2010**, *49*, 2167–2170.

[16] Q. Yuan, Y. Zhang, T. Chen, D. Lu, Z. Zhao, X. Zhang, Z. Li, C. H. Yan, W. Tan, *ACS Nano* **2012**, *6*, 6337–6344.

[17] G. K. Joshi, K. N. Blodgett, B. B. Muhoberac, M. A. Johnson, K. A. Smith, R. Sardar, *Nano Lett.* **2014**, *14*, 532–540.

[18] M. D. Pierschbacher, E. Ruoslahti, *Nature* **1984**, 3–6.

[19] D. Y. Wong, T. Ranganath, A. M. Kasko, *PLoS One* **2015**, *10*, 1–21.

[20] E. K. F. Yim, E. M. Darling, K. Kulangara, F. Guilak, K. W. Leong, *Biomaterials* **2010**, *31*, 1299–1306.

[21] F. Kantawong, K. E. V. Burgess, K. Jayawardena, A. Hart, R. J. Burchmore, N. Gadegaard, R. O. C. Oreffo, M. J. Dalby, *Biomaterials* **2009**, *30*, 4723–4731.

[22] A. K. Kundu, A. J. Putnam, *Biochem. Biophys. Res. Commun.* **2006**, *347*, 347–357.

[23] A. R. Cameron, J. E. Frith, J. J. Cooper-White, *Biomaterials* **2011**, *32*, 5979–5993.

[24] A. S. Rowlands, P. A. George, J. J. Cooper-White, *Am. J. Physiol. - Cell Physiol.* **2008**, *295*, 1037–1044.

[25] A. J. Engler, S. Sen, H. L. Sweeney, D. E. Discher, *Cell* **2006**, *126*, 677–689.

[26] J. E. Frith, R. J. Mills, J. J. Cooper-White, *J. Cell Sci.* **2012**, *125*, 317–327.

[27] K. A. Kilian, B. Bugarija, B. T. Lahn, M. Mrksich, *PNAS* **2010**, *107*, 4872–4877.

[28] M. A. Wozniak, K. Modzelewska, L. Kwong, P. J. Keely, *Biochim. Biophys. Acta - Mol. Cell Res.* **2004**, *1692*, 103–119.

[29] J. L. Bays, K. A. DeMali, *Cell. Mol. Life Sci.* **2017**, *74*, 2999–3009.

[30] J. D. Humphries, M. R. Chastney, J. A. Askari, M. J. Humphries, *Curr. Opin. Cell Biol.* **2019**, *56*, 14–21.

[31] T. Izard, D. T. Brown, *J. Biol. Chem.* **2016**, *291*, 2548–2555.

10.1002/anie.202105425

Entry for the Table of Contents

FULL PAPER

We created a photoswitchable DNA polymer containing azobenzene moieties and dynamically regulated the spatial distance between adhesion peptides with photoirradiation. Using the mechanical properties of this DNA polymer, UV and visible light irradiation induced the significant morphology change of the cells. This study presents a general strategy to explore nanoscale interactions between stem cells and stimuli responsive DNA nanostructures.

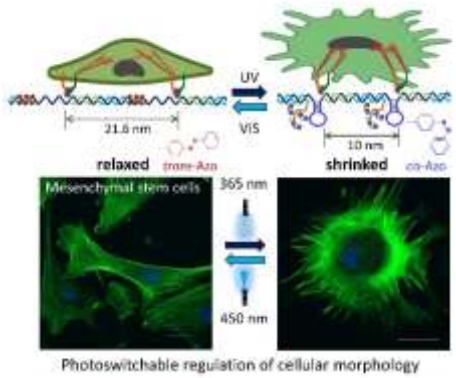

Photoswitchable regulation of cellular morphology

Soumya Sethi, Kumi Hidaka, Hiroshi Sugiyama, and Masayuki Endo**

Page No. – Page No.

Spatial and Temporal Regulation of Cellular Morphology Using a Photoswitchable Mechanical DNA Polymer